Chemical Engineering Journal 154 (2009) 231–235

Contents lists available at ScienceDirect

Chemical Engineering Journal

journal homepage: www.elsevier.com/locate/cej

Improvement of calcium fluoride crystallization by means of the reduction of fines formation

A. Garea*, R. Aldaco, A. Irabien

Departamento de Ingeniería Química y Química Inorgánica, ETSII y T, Universidad de Cantabria, Avda. Los Castros, s/n, 39005 Santander, Spain

ARTICLE INFO

Article history:
Received 22 December 2008
Received in revised form 10 April 2009
Accepted 21 April 2009

Keywords:
Fluoride control
Calcium fluoride
Crystallization
Supersaturation

ABSTRACT

This work focuses on fluoride recovery as a solid product CaF_2 in order to (i) improve process efficiency by means of the reduction of fines formation with the distributed feeding of calcium along the height of the reactor when high fluoride concentrations have to be treated; and (ii) to correlate the supersaturation effect on the fines formation and the process efficiency for the fluoride recovery as synthetic calcium fluoride.

An estimation of two parameters related to the product growth and the fines formation equations was performed in order to predict the process efficiencies in terms of fluoride removal and recovery as a solid product. The process simulation also provided the description of the crystallization process carried out in the tubular reactor contributing to the design and operation purposes for industrial applications of the fluoride control with recovery of solid product recovery as synthetic CaF_2 in pellet form available for industrial use.

1. Introduction

The limited natural resources of fluorspar, calcium fluoride, and the world consumption of fluorspar for chemical production, stabilising at around 4 million tons in 2004 (World Mineral Statistics, 2004) require that an effort be made to achieve sustainable management of the raw material as well as valorizing and including recycling in the production processes.

The fluoride recovery process to obtain synthetic calcium fluoride consists of a crystallization process in a fluidized bed reactor, which is proposed as an alternative to the conventional precipitation in the BREF document on Best Available Technology in common waste water and waste gas treatment and management systems in the Chemical Sector (European Commission, 2003).

The objective of the crystallization process under fluidized conditions is to achieve the fluoride removal requirement for the waste water disposal as well as the fluoride recovery as synthetic CaF_2 in the form of pellets available for industrial use: (i) reuse as raw material for the HF production (acid grade fluorspar: 97% CaF_2); (ii) filler material in concrete, enamels for ceramic substrates (ceramic grades fluorspar: 85–97% CaF_2), (iii) flux in the manufacture of steel and cast iron (metallurgical grade fluorspar: 60–85% CaF_2).

Previous works were focused on the study of the fluoride removal and recovery as synthetic CaF_2 by crystallization in a fluidized bed reactor working with standard fluoride solutions at laboratory scale [1–3], and the pilot plant scale operated with industrial waste waters [4].

A model of crystal growth of calcium fluoride was reported by Aldaco et al. [5–7], from the fitting of growth rate data to the variables: supersaturation, seed particle size, and superficial velocity in the fluidized bed. The crystal growth model was based on the aggregation and molecular growth mechanisms, while the nucleation process related to fines formation was described by a nucleation rate equation as a function of the supersaturation with well correlated data [7].

Low supersaturation values are related to nucleated precipitation, molecular growth and aggregation on the seed grains; while discrete precipitation, primary nucleation, is favored when the process is operated at higher supersaturation levels, leading to the formation of many nuclei which are not possible to be retained in the reactor, not even by aggregation with the seed particles. Under these conditions, the efficiency of the process decreases and the turbidity of the effluent increases.

As fines formation leads to a reduction of the process efficiency in terms of the amount of crystallization product recovered in the reactor, it is important to focus on the understanding of the mechanisms of fines formation in order to minimize this effect, mainly by means of the control of supersaturation.

Using the concept of distribution of local supersaturation along the reactor, achieved by multiple feed points, Costodes et al. [8] reported results of crystallization efficiencies up to 94% for the nickel hydroxy-carbonate recovery. The efforts made to understand of the mechanisms involved in the fluidized bed were also refer-

---

* Corresponding author. Tel.: +34 942201588; fax: +34 942201591.
E-mail address: gareaa@unican.es (A. Garea).

1385-8947/$ – see front matter © 2009 Elsevier B.V. All rights reserved.
doi:10.1016/j.cej.2009.04.050

Table 1
Main experimental data of the fluoride control and recovery in the reactors used at laboratory and pilot scales.

Reactor	Seed load (kg)	F^- in reactor (mg/l)	X	XF	XR	F^- out reactor (mg/l)
LAB1 (0.11 l,0.02 × 0.35 m)	0.07	150	0.91	0.19	0.72	15
		500	0.86	0.30	0.56	26
LAB2 (0.3 l, 0.02 × 1 m)	0.14	150	0.91	0.23	0.68	14
		500	0.96	0.45	0.51	22
		500 (3)	0.98	0.31	0.67	13
PILOT (0.26 m^3, 0.3 × 3 m)	20	150	0.88	0.18	0.7	18
	70	150	0.91	0.16	0.75	13
	22	300	0.95	0.43	0.52	14

enced for the removal of phosphorous [9,10], borax decahydrate [11], calcite and calcium fluoride [6,12,13].

Taking into account these previous studies on crystallization processes in fluidized bed reactors, the focus of this work is on fluoride recovery as solid product CaF_2 in order to (i) improve process efficiency by means of the reduction of fines formation, and (ii) be able to describe the effect of the distribution of the supersaturation, with the introduction of the product growth model and the fines formation equation so that the process efficiencies in terms of fluoride removal and recovery as solid product may be predicted.

2. Experimental section

The operation of the crystallization process was carried out at laboratory scale, by using two fluidized bed reactors (one prepared for the distributed feeding of calcium from hydrated lime solution, Fig. 1), and at pilot scale working in this case with industrial fluoride waste water (capacity 5 $m^3\,h^{-1}$, operated with 3 $m^3\,h^{-1}$ [4]).

Samples were taken during each experiment at different time intervals for the measurement of fluoride dissolved, pH and concentration of fines in the outlet stream. Dissolved fluoride was analyzed by a specific fluoride ion electrode provided with a reference electrode. The concentration of fines as suspended solids in the outlet stream was calculated from filtration (0.45 μm filter) of samples and determination of the cake weight.

Table 1 summarises the main data corresponding to the operation in the reactors, the dimensions of each reactor, seed load (industrial $CaCO_3$) and fluoride concentration at the inlet (bottom, at the first point of contact between the fluoride and calcium streams) and at the outlet of the reactor; and the results calculated from the measured variables are shown in terms of process efficiency (X, as total fluoride removal fraction), conversion to solid product (XR, as synthetic CaF_2), and fraction of fluoride lost as fines to the outlet stream (XF), defined as follows

$$X = \frac{w_{\mathrm{F,bottom\ reactor}} - w_{\mathrm{F,out\ reactor}}}{w_{\mathrm{F,bottom\ reactor}}} \tag{1}$$

$$XR = \frac{w_{\mathrm{F,grains\ product}}}{w_{\mathrm{F,bottom\ reactor}}} \tag{2}$$

$$XF = \frac{w_{\mathrm{F,\,fines}}}{w_{\mathrm{F,\,bottom\ reactor}}} \tag{3}$$

being

$$X = XR + XF \tag{4}$$

where $w_{\mathrm{F,bottom\ reactor}}$ and $w_{\mathrm{F,out\ reactor}}$ are the fluoride molar flowrates, at the bottom of the reactor (first point of contact with the calcium stream) and at the outlet of the reactor in the filtered samples; $w_{\mathrm{F,\ grains\ product}}$ is the fluoride molar flowrate as product recovered from the reactor (synthetic CaF_2), and $w_{\mathrm{F,\ fines}}$ is the fluoride molar flowrate as small particles contained in the outlet stream of the reactor.

It should be noted that in Table 1 the row related to the experiments (three replicates) operated with a relative high concentration of fluoride, 500 $mg\,l^{-1}$, with three points of calcium along the reactor in order to study the effect of the local supersaturation on the fraction of fines.

The supersaturation can be defined for the calcium fluoride system at room temperature [2] as

$$S = \left[\frac{[Ca^{2+}][F^-]^2}{3.4\,10^{-11}}\right] \tag{5}$$

During the experiments, the increase in height of the fluidized bed in the reactor was also measured, as it is shown in Fig. 2, and the CaF_2 content in the growing particles was estimated from time zero when the seed particles of $CaCO_3$ were loaded (325 μm of mean diameter size, density 2.66 $g\,cm^{-3}$, Calcinor, S.A.).

3. Improvement of process efficiency by multiple feed points of calcium

For an industrial application, production of fines must be minimized since they can be elutriated out of the bed when the superficial velocity through the bed exceeds their terminal velocity.

Potential sources of fines in the fluidized bed are: homogeneous nucleation due to high supersaturation at feed points [14], attrition as a result of collisions occurring in the bed and lastly dissolution of larger particles to form smaller ones.

In order to control the distribution of the supersaturation throughout the bed, the local supersaturation was changed by changing the number of feed points of calcium to the reactor, from one inlet point at the bottom up to three inlet points equally spaced along the bed.

It can be observed from the results of XR and XF at different inlet fluoride concentrations that the conversion of fluoride to solid product in the reactor is affected by this variable (Table 1), when higher fluoride concentrations are treated lower product recovery (XR) is achieved and a higher amount of fluoride is lost as fine particles in the exit stream (XF).

From the results obtained it can be observed that there is a decrease in fines in terms of XF, 0.31 fraction compared to 0.45 fraction when only one point of calcium feeding is working at the same fluoride concentration (500 $mg\,l^{-1}$). The decrease in fines fraction leads to higher conversion to solid product, 0.51 to 0.67, as CaF_2 which remains in the reactor during the operation and it is recovered for reuse when the operating cycle indicates stop (controlled by an allowable maximum pressure drop).

Fig. 3 shows the effect of the multiple inlet points of calcium on the local supersaturation and the fraction of fines determined at each point along the bed. The supersaturation values are represented as relative respect to the supersaturation value at the inlet point at the bottom of the reactor (height $H = 0$).

From the results obtained, the distributed supersaturation along the bed in order to decrease the fraction of fines, as

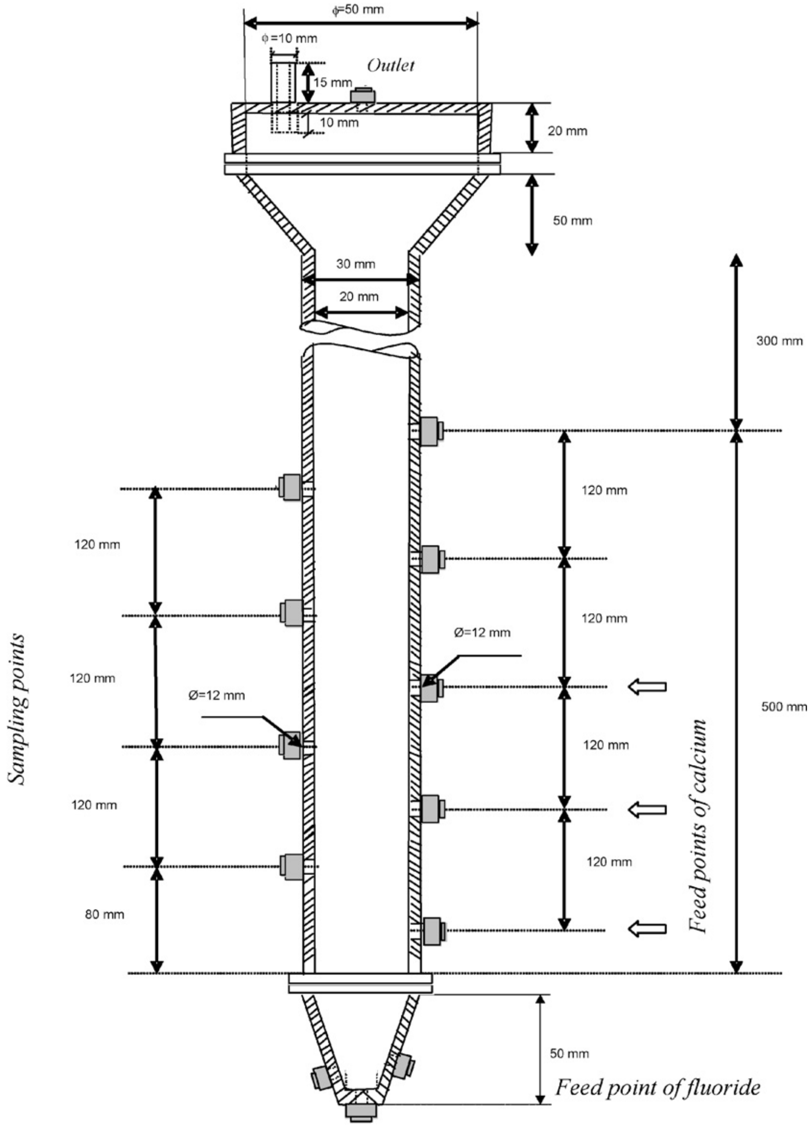

Fig. 1. Scheme of the laboratory reactor with multiple inlets of calcium streams.

is shown when three inlets of calcium were operated, can be seen to have a significant effect, with the values of fines local fraction varying from 0.4 (at the bottom of the reactor, considered height $H = 0$, first point of contact between calcium and fluoride solutions) to 0.05 at the exit of the reactor (height, $H = 1$ m).

4. Simulation of the crystallization process: product pellets and fines growth Rates

In order to describe the crystallization process of synthetic CaF_2, the mass balances for fluoride and calcium have to be solved in conjuntion with the equations of product (grains) growth and fines

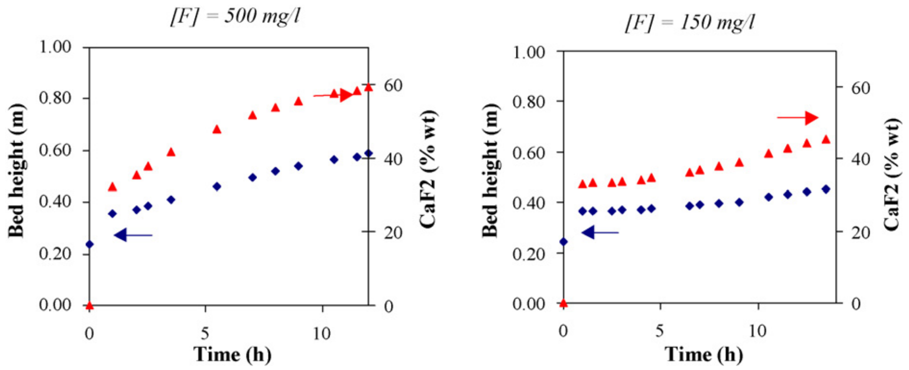

Fig. 2. Trends of bed height and CaF_2 purity (%) during the operation time for fluoride concentrations of 500 and 150 mg l^{-1} at the bottom of reactor.

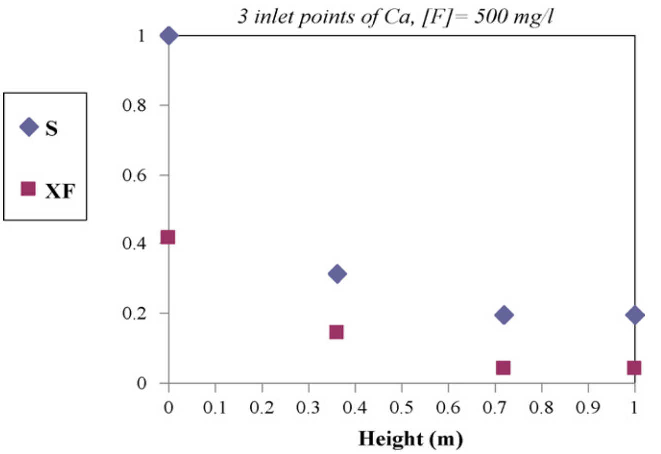

Fig. 3. Effect of 3 inlet points of calcium to local relative supersaturation and fraction of fines along the bed height when 500 mg l^{-1} fluoride is treated.

formation along the bed during the operation time. The Zaki equations were used for the description of bed porosity and pressure drop as functions of the discretizated variables diameter and density of the growing particles along the bed, in terms of Reynolds particle number and terminal velocity.

The particle growth equation (Eq. (6)), was proposed as overall linear growth rate, G, based on the aggregation and molecular growth mechanisms from previous studies with accurate fitting to experimental data at laboratory scale [6] in the studied range of variables, superficial velocity (SV), particle size of the seed material (Lo), and supersaturation (S)

$$G = (k_1 + k_2\mathrm{Lo}^2)\mathrm{SV}^{0.5}S^{n} \tag{6}$$

considering the relationship between the crystal growth rate expressed as mass deposition, R_G, and the overall linear growth rate as the change in a characteristic dimension on the crystal per time unit, G

$$R_G = \frac{1}{A}\frac{dM}{dt} = 3\frac{\alpha}{\beta}\rho\frac{dL}{dt} \tag{7}$$

where L is a characteristic size of the crystal, α and β the volume and surface shape factors, and ρ the crystal density.

The formation of fines as a function of the supersaturation was described by the following Eq. (8) taking into account the well correlated data reported from previous studies at laboratory scale [7]

$$r_F = k_F \exp\left(-\frac{C_s}{(\ln S)^2}\right) \tag{8}$$

Introducing the data obtained in the present work, at laboratory and pilot scales, and with three inlet points of calcium to the fluidized bed in order to analyze the effect of the distributed supersaturation variable, the global estimation of two parameters was carried out. The estimated parameters are related with the supersaturation dependence of the particle growth equation, given as a potential dependence of S in Eq. (6), S^n, and the kinetic constant of the Eq. (8) for fines formation, k_F, considering that the effect of the distributed supersaturation in the fines formation fraction.

Table 2
Estimated parameters for fitting the particle growth and fines formation equations.

n	2/3
k_F	26 (mg s^{-1} l^{-1})
Mean global error (%)	12%

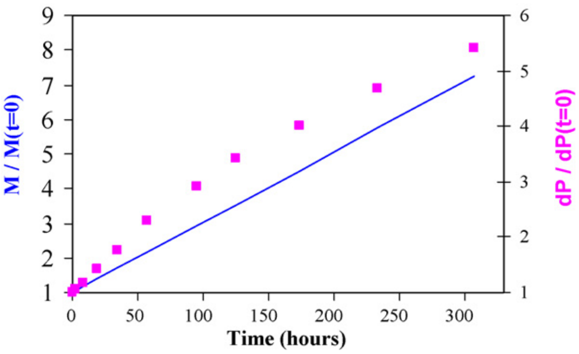

Fig. 5. Simulation results of the mean dimensionless mass of product and pressure drop for long operational times.

Table 2 shows the results of the estimated parameters, n (from Eq. (6)) and k_F (from Eq. (8)), as well as the mean global error (%) of the simulated results respect to the experimental data (laboratory and pilot scales) of four variables: fluoride dissolved at the outlet stream, and the fractions X, XR, XF. The value of the mean error was 12% for the global simulation of the total amount of data (laboratory and pilot scales).

The software used for the estimation and simulation tasks is the custom modelling language of Aspen Custom Modeler (Aspentech).

The simulation of the process operation is also shown in Figs. 4 and 5: Fig. 4 summarises the simulated trends over time of some variables, particle diameter and porosity of the bed, at 10 nodes of the discretizated height of the reactor (H = 1 being at the top, the outlet of the reactor); Fig. 5, though, shows the simulated trends of the dimensionless variables: total mass of particles growing in the bed and the corresponding total pressure drop which is used as the control variable for the operation cycle.

From the simulation tool, the behaviour of the crystallization process carried out in the tubular reactor is described, contributing

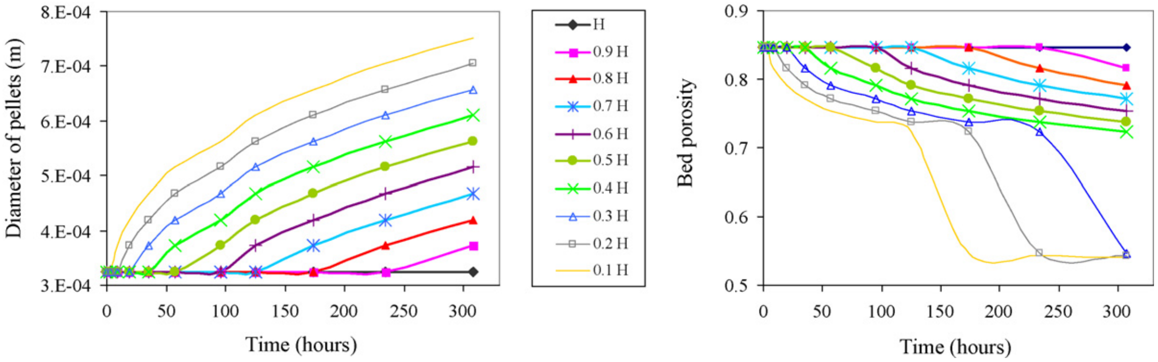

Fig. 4. Simulation results of the distributed diameter of pellets and bed porosity at 10 nodes along reactor height for long operational times.

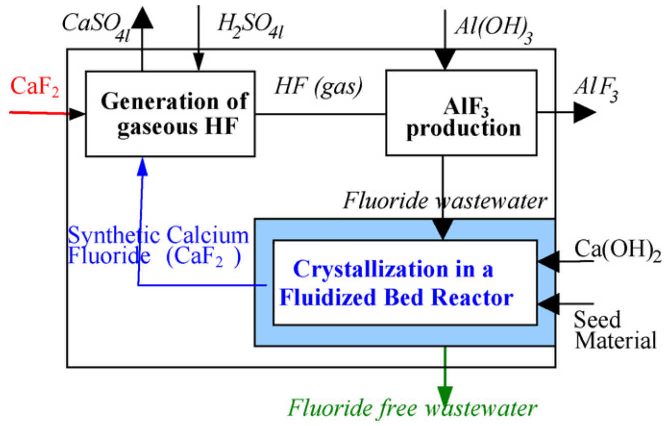

Fig. 6. Scheme of HF and AlF_3 production with integration of raw material by fluidized crystallization (CaF_2).

to the design and operation purposes for industrial applications of the fluoride control and recovery as solid product to be reused as synthetic CaF_2 in pellet form available for industrial use: (i) reuse as raw material for the HF production as is shown in Fig. 6 (if 97% CaF_2 is achieved, as the required acid grade fluorspar); (ii) filler material in concrete, enamels for ceramic substrates (ceramic grades fluorspar: 85–97% CaF_2), (iii) flux in the manufacture of steel and cast iron (metallurgical grade fluorspar: 60–85% CaF_2).

5. Conclusions

The experimental results of process efficiency at laboratory scale indicated a significant increase of 30% when three feed points of calcium where used in comparison to one point at the bottom of the reactor, working with a fluoride concentration of 500 mg l^{-1} at the inlet of the reactor. It is important to remark that with the use of the distribution of local supersaturation, it is possible a better control of the supersaturation in the bed and, therefore, the production of fine particles that reduce process efficiency.

The process simulation also provided us with an estimation of the benefits of the consumption of raw materials and waste disposal, and it is used as an important tool to scale up the process for its integration into the production lines.

Acknowledgments

This research is financially supported by the Spanish Ministry of Science and Technology (Project CONSOLIDER CTM2006-00317). The authors gratefully acknowledge the support of Derivados del Flúor S.A. (Ontón, Cantabria) for the pilot plant collaboration.

References

[1] A. Irabien, A. Garea, R. Aldaco, O. Perez, J.M. Saenz, Patent number ES2270705, 01/04/2007.
[2] R. Aldaco, P. de Luis, A. Irabien, Fluidized bed reactor for fluoride removal, Chem. Eng. J. 107 (2005) 113–117.
[3] R. Aldaco, A. Garea, A. Irabien, Calcium fluoride recovery from fluoride wastewater in a fluidized bed reactor, Water Res. 41 (2007) 810–818.
[4] A. Garea, R. Aldaco, E. Lopez, A. Irabien, Pilot plant operation of a fluidized crystallization process for calcium fluoride recovery, 5th European Meeting on Chemical Industry and Environment, Vienna, 2006.
[5] R. Aldaco, A. Garea, A. Irabien, Modelling of particle growth: application to water treatment in a fluidized bed reactor, Chem. Eng. J. 134 (2007) 66–71.
[6] R. Aldaco, A. Garea, A. Irabien, Particle growth kinetics of calcium fluoride in a fluidized bed reactor, Chem. Eng. Sci. 62 (2007) 2958–2966.
[7] R. Aldaco, A. Garea, A. Irabien, Fluoride recovery in a fluidized bed: crystallization of calcium fluoride on silica sand, Ind. Eng. Chem. Res. 45 (2006) 796–802.
[8] V.C. Costodes, A.E. Lewin, Reactive crystallization of nickel hydroxy-carbonate in fluidized-bed reactor: fines production and column design, Chem. Eng. Sci. 61 (2006) 1377–1385.
[9] M.M. Seckler, O.S.L. Bruinsma, G.M. van Rosmalen, Phosphate removal in a fluidized bed- I. Identification of physical processes, Water Res. 30 (1996) 1585–1588.
[10] P. Battistoni, A. Deangelis, P. Pavan, M. Prisclandaro, F. Cecchi, Phosphorous removal from a real anaerobic supernatant by struvite crystallization, Water Res. 35 (2001) 2167–2178.
[11] A.A. Ceyhan, O. Sahin, A.N. Bulutcu, Crystallization kinetics of the borax decahydrate, J. Crystal Growth 300 (2007) 440–447.
[12] C.Y. Tai, M.-C. Chang, C.-K. Wu, Y.-C. Lin, Interpretation of calcite growth data using the two step crystal growth model, Chem. Eng. Sci. 61 (2006) 5346–5354.
[13] C. Tai, P.C. Chen, T.M. Tsao, Growth kinetics of CaF_2 in a pH-stat fluidized-bed crystallizer, J.Crystal Growth 290 (2006) 576–584.
[14] J. Garside, Industrial Crystallization from solution, Chem. Eng. Sci. 40 (1985) 3–26.